AIMS Mathematics, 7(9): 16296–16314.
DOI: 10.3934/math.2022890
Received: 30 March 2022
Revised: 15 June 2022
Accepted: 28 June 2022
Published: 04 July 2022

http://www.aimspress.com/journal/Math

Research article

Impact of the strong Allee effect in a predator-prey model

Yudan Ma[1], **Ming Zhao**[1,*] **and Yunfei Du**[2]

[1] School of Science, China University of Geosciences (Beijing), Beijing 100083, China
[2] School of Basic Education, Beijing Institute of Graphic Communication, Beijing 102600, China

* **Correspondence:** Email: mingzhao@cugb.edu.cn.

Abstract: In this work, we propose and investigate a new predator-prey model with strong Allee effect in prey and Holling type II functional response in predator. By performing a comprehensive dynamical analysis, we first derive the existence and stability of all the possible equilibria of the system and the system undergoes two transcritical bifurcations and one Hopf-bifurcation. Next, we have calculated the first Lyapunov coefficient and find the Hopf-bifurcation in this model is supercritical and a stable limit cycle is born. Then, by comparing the properties of the system with and without Allee effect, we show that the strong Allee effect is of great importance to the dynamics. It can drive the system to instability. Specifically, Allee effect can increase the extinction risk of populations and has the ability to switch the system's stability to limit cycle oscillation from stable node. Moreover, numerical simulations are presented to prove the validity of our findings.

Keywords: predator-prey model; Allee effect; transcritical bifurcation; Hopf-bifurcation
Mathematics Subject Classification: 34C23, 92D25, 34D20, 65P40

1. Introduction

In the field of mathematical ecology, mathematical models are extensively used to explore and describe the complex interactions among individuals and between individuals and their surroundings by many scholars [1–5]. Especially, the predator-prey models have received great attention over the last one hundred years. Since the classical two species Lotka-Volterra model was put forward [1], there are a great many of experiments and papers investigating the interactions between predators and prey from each aspect [6–10]. Such as, in [7] the authors studied the complex dynamics of a predator-prey model with the nonlinear Michaelis-Menten type predator harvesting. Li et al. [8] proposed a Leslie-Gower predator-prey model with simplified Holling-type IV functional response. In [10] S. Djilali and S. Bentout proposed a delayed diffusive predator-prey model with prey social behavior and predator harvesting, and analyzed the dynamics of the deterministic model and diffusive model.

In recent years, it is widely recognized the Allee effect has important significance on the population dynamical relation and may make the dynamics more richer. Specifically, Allee effect refers to a positive correlation between population density and individual average fitness when the population is small [11, 12]. From the view point of ecology, Allee effect on species can occur under some mechanisms, such as the change of habitat, inbreeding depression, difficulties in finding a spouse, avoiding predators, and the predation risk caused by environment conditions [13–15]. Moreover, the Allee effect is mainly divided into two forms: Strong and weak [16]. The strong Allee effect denotes the negative per capita growth rate when population density is below the so-called Allee threshold and the growth rate becomes positive when the population density is above this threshold [17]. This means, the population must surpass the threshold to grow. Contrarily, a population with a weak Allee effect has no such above threshold and the weak Allee effect means that when the species density is low, the per capita growth rate becomes small, but remains positive [18, 19]. This implies the Allee effect may lead to much more complex dynamics and thereby affect the survival of the population. In fact in [20], Hilker et al. have introduced the strong Allee effect in a simple epidemic model [21, 22] and shown that Allee effect can induce surprisingly rich dynamical behaviors, like periodic oscillations, multiple alternative steady states and homoclinic loops with the extinction of host populations. The complexity reveals, the introduction of the Allee effect in mathematical systems has important practical significance to the study of long-term species morphology and the development of species. This could have far-reaching implications in areas of biological protection.

On the other hand, there is another key objective that can also affect the dynamical behaviors of the prey-predator models: Functional response [23]. It refers to the average number of prey killed by each individual predator per unit of time and has two main types: Predator-dependent (as a function of prey and predators densities) and prey-dependent (as a function of the prey density) [24]. Exactly, functional response denotes the latter, like the famous Holling family [25], plays a predominant role in species dynamics models. For instance, since 1965, Holling's type II functional response has acted as the basis for many literatures [26–30] on predator-prey theory.

Specially, for insect pest management, in [28] Sun et al. considered a prey-predator system with Holling type II functional response in the predator:

$$\begin{cases} \frac{dx}{dt} = x(r - \frac{rx}{K} - by), \\ \frac{dy}{dt} = y\left(\frac{\lambda bx}{1+bhx} - d_1\right), \end{cases} \tag{1.1}$$

where $x(t)$ and $y(t)$ denote the population densities of prey and predator at time t, respectively. r is the growth rate of $x(t)$, K is the environment capacity in the absence of predator. $\frac{bx}{1+bhx}$, which is assumed to be the typical Holling type II functional response form, gives a description of the per capita conversion rate from prey to predator. Concretely, b and h represent the searching rate and handling time of predator, λ denotes the conversion efficiency. All the parameters are positive. By dynamical analysis, Sun et al. [28] concluded if $0 \le h \le \frac{\lambda}{d_1}$, system (1.1) has two saddles $P_0(0, 0)$, $P_1(K, 0)$, and a globally asymptotically stable focus $P_3\left(\frac{d_1}{b(\lambda - hd_1)}, \frac{r(Kb(\lambda - hd_1) - d_1)}{Kb^2(\lambda - hd_1)}\right)$.

Thus, motivated by the above discussion, we naturally want to know: When an Allee effect is subject to the first species of system (1.1), what will happen to the dynamical properties? Hence, we construct the following ecological model with a strong Allee effect in prey

$$\begin{cases} \frac{dx}{dt} = x(r - \frac{rx}{K})(x - A) - bxy, \\ \frac{dy}{dt} = y\left(\frac{\lambda bx}{1+bhx} - d_1\right), \end{cases} \tag{1.2}$$

where A is the strong Allee effect parameter and it satisfies $0 < A < K$ and other parameters are the same as system (1.1). Let $\bar{t} = Krt$, $\bar{x} = \frac{1}{K}x$ and $\bar{y} = \frac{b}{r}y$, and drop the bars, we get

$$\begin{cases} \frac{dx}{dt} = x(1-x)(x-\alpha) - \frac{1}{K}xy, \\ \frac{dy}{dt} = y\left(\frac{\omega x}{1+\eta x} - \sigma\right), \end{cases} \tag{1.3}$$

where $\alpha = \frac{A}{K}$, $\omega = \frac{\lambda b}{r}$, $\sigma = \frac{d_1}{Kr}$, $\eta = bhK$, and the strong Allee effect parameter α taken as $0 < \alpha < 1$.

Our main purpose aims to see how the strong Allee effect affect the dynamics of the prey-predator model with Holling type II functional response. The layout of this paper is as follows. First, the positivity and boundedness of solution of system (1.3) are studied in Section 2. Then, in Section 3, we give the analysis of equilibria of system (1.3), including the distribution of all the possible equilibria and their stability. In Section 4, we verify the existence of transcritical bifurcation and Hopf-bifurcation. Additionally, numerical simulations and computations are carried out to explore and visualize the impact of the strong Allee effect in Section 5. Finally, this paper is concluded with a brief summary in Section 6.

2. Preliminaries

Next, the positivity and boundedness of the solutions of system (1.3) will be shown in the region $\mathbb{R}^2_+ = \{(x, y) : x \geq 0, y \geq 0\}$.

2.1. Positivity

Lemma 2.1. *For all $t \geq 0$, every solution of system* (1.3) *with initial value is positive.*

Proof. Solving system (1.3) with positive initial condition $(x(0), y(0))$, we get the result:

$$x(t) = x(0)\left[\exp\int_0^t \left((1-x(s))(x(s)-\alpha) - \frac{1}{K}y(s)\right)ds\right] > 0,$$
$$y(t) = y(0)\left[\exp\int_0^t \left(\frac{\omega x(s)}{(1+\eta x(s))} - \sigma\right)ds\right] > 0.$$

Hence, any solution of system (1.3) starting from the interior of the first quadrant xy-plane still remains in it for all future times.

2.2. Uniform boundedness

Lemma 2.2. *Every solution of system* (1.3) *with positive initial value is uniformly bounded.*

Proof. Let $\Phi = K\omega x + y$ and $\delta = \min\{\alpha, \sigma\}$, we have

$$\begin{aligned} \frac{d\Phi}{dt} + \delta\Phi &= K\omega\left[x(1-x)(x-\alpha) - \frac{1}{K}xy\right] + \frac{\omega xy}{1+\eta x} - \sigma y + \delta K\omega x + \delta y \\ &\leq -K\omega x^3 + K\omega(1+\alpha)x^2 - K\omega(\alpha-\delta)x - (\sigma-\delta)y \\ &\leq -K\omega x^3 + K\omega(1+\alpha)x^2 \leq \frac{4K\omega(1+\alpha)^3}{27} \triangleq \varrho. \end{aligned}$$

Integrating the above inequality, we have $\Phi(t) \leq e^{-\delta t}\Phi(0) + \frac{\varrho}{\delta}(1 - e^{-\delta t})$ and $\limsup \Phi(t) \leq \varrho\delta^{-1}$, as $t \to \infty$, independently of the initial conditions. Therefore, the solutions of system (1.3) are uniformly bounded.

Remark 2.1. From the perspective of ecology, uniform boundedness of system (1.3) means that the interacting two species are ecologically well behaved and none of them can grow exponentially for a long period of time owing to limited food sources.

3. Equilibria and stability analysis

3.1. Existence of equilibria

Obviously, for all permissible parameters, system (1.3) always has three boundary equilibria $E_0(0, 0)$, $E_1(1, 0)$ and $E_2(\alpha, 0)$. If system (1.3) admits the positive equilibrium, then x and y must satisfy the equation as follows:

$$\begin{cases} (1 - x)(x - \alpha) - \frac{y}{K} = 0, \\ \frac{\omega x}{1+\eta x} - \sigma = 0. \end{cases} \tag{3.1}$$

By some simple algebraic calculations, we obtain the system has a unique positive equilibrium $E_3\left(\frac{\sigma}{\omega-\sigma\eta}, \frac{K(\omega-(\eta+1)\sigma)(\sigma-\alpha(\omega-\sigma\eta))}{(\omega-\sigma\eta)^2}\right)$ for $\frac{\omega\alpha}{1+\eta\alpha} < \sigma < \frac{\omega}{1+\eta}$.

3.2. Stability of equilibria

Theorem 3.1. *The trivial equilibrium E_0 is a hyperbolic stable node.*

Proof. The Jacobian matrix at $E_0(0, 0)$ is given by

$$J_{E_0} = \begin{pmatrix} -\alpha & 0 \\ 0 & -\sigma \end{pmatrix}, \tag{3.2}$$

which, clearly, has two negative eigenvalues $\lambda_1(E_0) = -\alpha < 0$ and $\lambda_2(E_0) = -\sigma < 0$. Hence, the extinction equilibrium E_0 in the first quadrant is always a stable node.

Theorem 3.2. *For the boundary equilibrium E_1:*

(*i*) *if $\sigma < \frac{\omega}{1+\eta}$, then E_1 is a hyperbolic saddle;*

(*ii*) *if $\sigma = \frac{\omega}{1+\eta}$, then E_1 is a non-hyperbolic saddle node. It means $S_\epsilon(E_1)$ is divided into two parts by two separatrices that tend to E_1 along the left and the right of E_1, where $S_\epsilon(E_1)$ is a neighborhood of E_1 with sufficient small radius ϵ. One part consists of two hyperbolic sectors and another is a parabolic sector which is on the upper half plane.*

(*iii*) *if $\sigma > \frac{\omega}{1+\eta}$, then E_1 is a stable node.*

Proof. The corresponding Jacobian matrix at $E_1(1, 0)$ is calculated as follows:

$$J_{E_1} = \begin{pmatrix} \alpha - 1 & -\frac{1}{K} \\ 0 & \frac{\omega}{1+\eta} - \sigma \end{pmatrix}, \tag{3.3}$$

with two eigenvalues $\lambda_1(E_1) = \alpha - 1 < 0$ and $\lambda_2(E_1) = \frac{\omega}{1+\eta} - \sigma$. Thus E_1 is a hyperbolic saddle if $\sigma < \frac{\omega}{1+\eta}$ and a stable node if $\sigma > \frac{\omega}{1+\eta}$ (see Fig.1(a) and (c)). For $\sigma = \frac{\omega}{1+\eta}$, namely, the eigenvalue $\lambda_2(E_1) = 0$ and E_1 is non-hyperbolic, so we can not judge its type from the eigenvalues directly. Below we will use Theorem 7.1 in Chapter 2 in [31] to discuss the stability properties of E_1.

By letting $(\bar{x}, \bar{y}) = (x - 1, y)$, we change system (1.3) into a standard form and then expand it to

$$\begin{cases} \frac{d\bar{x}}{dt} = (\alpha - 1)\bar{x} - \frac{1}{K}\bar{y} - (2 - \alpha)\bar{x}^2 - \frac{1}{K}\bar{x}\bar{y} - \bar{x}^3, \\ \frac{d\bar{y}}{dt} = c_1\bar{x}\bar{y} + c_2\bar{x}^2\bar{y} + c_3\bar{x}^3\bar{y} + Q_0(\bar{x}, \bar{y}), \end{cases} \tag{3.4}$$

where $c_1 = \frac{\omega}{(1+\eta)^2}$, $c_2 = -\frac{\omega\eta}{(1+\eta)^3}$, $c_3 = \frac{\omega\eta^2}{(1+\eta)^4}$, and $Q_0(\bar{x}, \bar{y})$ represents a power series with terms $\bar{x}^i\bar{y}^j$ $(i + j \geq 5)$.

By the linear transformation

$$\begin{pmatrix} \bar{x} \\ \bar{y} \end{pmatrix} = \begin{pmatrix} 1 & -1 \\ 0 & (1 - \alpha)K \end{pmatrix} \begin{pmatrix} u \\ v \end{pmatrix}, \tag{3.5}$$

then system (3.4) becomes

$$\begin{cases} \frac{du}{dt} = d_1u + d_2u^2 + d_3uv + d_4v^2 + d_5u^3 + d_6u^2v + d_7uv^2 + d_8v^3 + Q_1(u, v), \\ \frac{dv}{dt} = c_1uv - c_1v^2 + c_2u^2v - 2c_2uv^2 + c_2v^3 + Q_2(u, v), \end{cases} \tag{3.6}$$

where

$$d_1 = \alpha - 1,\ d_2 = -2 + \alpha,\ d_3 = -2\alpha + 3 - c_1,\ d_4 = -1 - c_1,$$
$$d_5 = -1,\ d_6 = c_2 - 3,\ d_7 = -3 - 2c_2,\ d_8 = c_2 - 1,$$

and $Q_1(u, v)$ and $Q_2(u, v)$ represent power series with terms $u^iv^j (i + j \geq 4)$.

Let $\tau = d_1t$, then system (3.6) becomes

$$\begin{cases} \frac{du}{d\tau} = u + \frac{d_2}{d_1}u^2 + \frac{d_3}{d_1}uv + \frac{d_4}{d_1}v^2 + \frac{d_5}{d_1}u^3 + \frac{d_6}{d_1}u^2v + \frac{d_7}{d_1}uv^2 + \frac{d_8}{d_1}v^3 + \frac{Q_1(u,v)}{d_1} \triangleq u + P(u, v), \\ \frac{dv}{d\tau} = \frac{c_1}{d_1}uv - \frac{c_1}{d_1}v^2 + \frac{c_2}{d_1}u^2v - \frac{2c_2}{d_1}uv^2 + \frac{c_2}{d_1}v^3 + \frac{Q_2(u,v)}{d_1} \triangleq Q(u, v). \end{cases} \tag{3.7}$$

From the implicit function theorem and $\frac{du}{d\tau} = 0$, we can obtain a unique function

$$u = \varphi_1(v) = -\frac{d_4}{d_1}v^2 + \frac{d_3d_4 - d_1d_8}{d_1^2}v^3 + \cdots,$$

which satisfies $\varphi_1(0) = \varphi_1'(0) = 0$ and $\varphi_1(v) + P(\varphi_1(v), v) = 0$. Then substituting it into the second equation of (3.7), we have that

$$\frac{dv}{d\tau} = -\frac{c_1}{d_1}v^2 - \frac{c_1d_4 - c_2d_1}{d_1^2}v^3 - \frac{c_1(d_3d_4 - d_1d_8) - 2c_2d_1d_4}{d_1^3}v^4 + O(|v|^5). \tag{3.8}$$

The coefficient of v^2 is $-\frac{c_1}{d_1} < 0$. Thus, by using Theorem 7.1 in Chapter 2 in [31], we get E_1 is a saddle node. This means that a neighborhood of $S_\varepsilon(E_1)$ is divided into two parts by two separatrices that tend to E_1 along the left and the right of E_1 (see Figure 1(b)). One part consists of two hyperbolic sectors and another is a parabolic sector which is on the upper half plane.

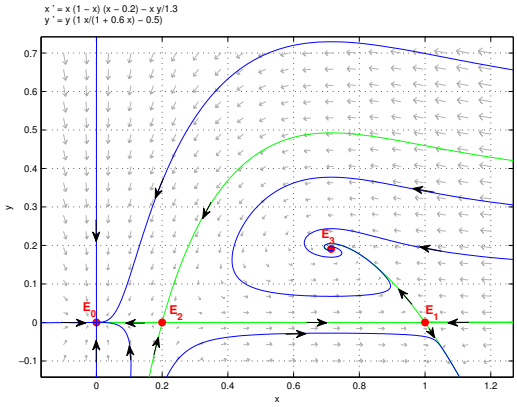

(a)

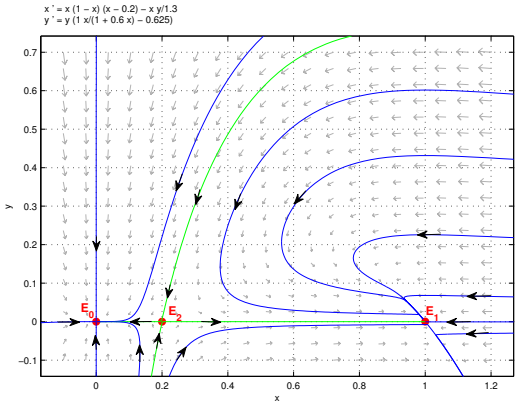

(b)

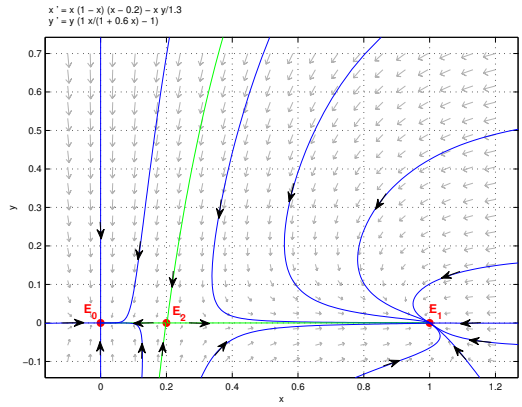

(c)

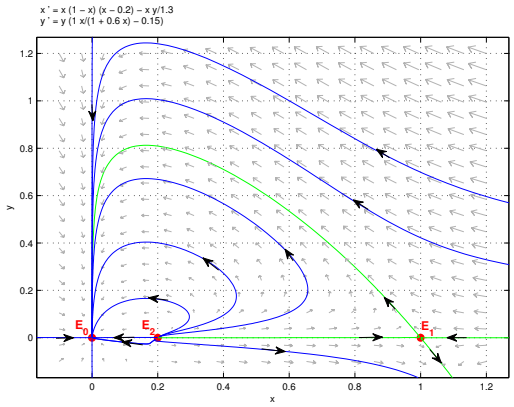

(d)

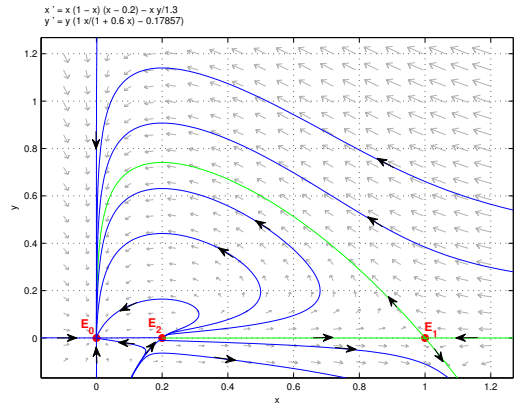

(e)

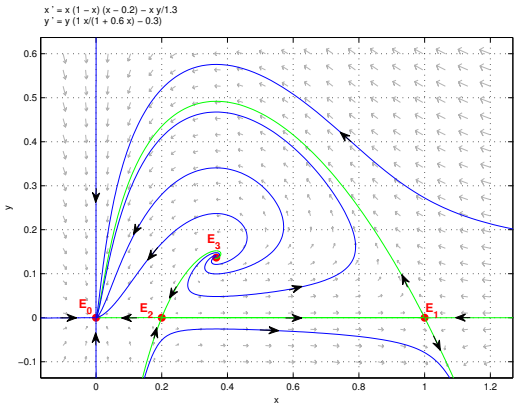

(f)

Figure 1. The phase portraits of system (1.3).

Theorem 3.3. *For the boundary equilibrium E_2:*

(*i*) *if $\sigma < \frac{\omega\alpha}{1+\eta\alpha}$, then E_2 is an unstable node;*
(*ii*) *if $\sigma = \frac{\omega\alpha}{1+\eta\alpha}$, then E_2 is a non-hyperbolic saddle node. This means $S_\epsilon(E_2)$ is divided into two parts by two separatrices that move away along the left and the right of E_2. One part consists of two hyperbolic sectors, and another is a parabolic sector which is on the upper half-plane;*
(*iii*) *if $\sigma > \frac{\omega\alpha}{1+\eta\alpha}$, then E_2 is a hyperbolic saddle.*

Proof. The Jacobian matrix J_{E_2} of $E_2(\alpha, 0)$ is

$$J_{E_2} = \begin{pmatrix} \alpha(1-\alpha) & -\frac{1}{K}\alpha \\ 0 & \frac{\omega\alpha}{1+\eta\alpha} - \sigma \end{pmatrix}. \tag{3.9}$$

Then the eigenvalues $\lambda_1(E_2) = \alpha(1-\alpha) > 0$ and $\lambda_2(E_2) = \frac{\omega\alpha}{1+\eta\alpha} - \sigma$. Clearly, E_2 is an unstable node if $\sigma < \frac{\omega\alpha}{1+\eta\alpha}$ and a saddle if $\sigma > \frac{\omega\alpha}{1+\eta\alpha}$ (see Figure 1(*d*) and (*f*)). However, when $\sigma = \frac{\omega\alpha}{1+\eta\alpha}$, the eigenvalue $\lambda_2(E_2) = 0$ which indicates E_2 is non-hyperbolic. In order to deduce its stability, we translate E_2 to the origin via the translation $(\bar{x}, \bar{y}) = (x - \alpha, y)$ and then expand system (1.3) to

$$\begin{cases} \frac{d\bar{x}}{dt} = (1-\alpha)\alpha\bar{x} - \frac{\alpha}{K}\bar{y} + (1-2\alpha)\bar{x}^2 - \frac{1}{K}\bar{x}\bar{y} - \bar{x}^3, \\ \frac{d\bar{y}}{dt} = f_1\bar{x}\bar{y} + f_2\bar{x}^2\bar{y} + M_0(\bar{x}, \bar{y}), \end{cases} \tag{3.10}$$

where $f_1 = \frac{\omega}{(1+\eta\alpha)^2}$, $f_2 = -\frac{\omega\eta}{(1+\eta\alpha)^3}$, and $M_0(\bar{x}, \bar{y})$ represents a power series in $(\bar{x}, \bar{y})$ with terms $\bar{x}^i\bar{y}^j(i + j \geq 4)$.

Let

$$T = \begin{pmatrix} 1 & 1 \\ 0 & K(1-\alpha) \end{pmatrix}$$

be an invertible matrix. We use the following linear transformation

$$\begin{pmatrix} u \\ v \end{pmatrix} = T \begin{pmatrix} \bar{x} \\ \bar{y} \end{pmatrix}, \tag{3.11}$$

then system (3.10) turns into

$$\begin{cases} \frac{du}{dt} = e_1u + e_2u^2 + e_3uv + e_4v^2 + e_5u^3 + e_6v^3 + e_7u^2v + e_8uv^2 + M_1(u, v), \\ \frac{dv}{dt} = f_1uv + f_1v^2 + f_2u^2v + 2f_2uv^2 + f_2v^3 + M_2(u, v), \end{cases} \tag{3.12}$$

where $e_1 = (1-\alpha)\alpha$, $e_2 = 1 - 2\alpha$, $e_3 = 1 - 3\alpha - f_1$, $e_4 = -\alpha - f_1$, $e_5 = -1$, $e_6 = f_2 - 1$, $e_7 = f_2 - 3$, and $e_8 = 2f_2 - 3$. $M_1(u, v)$ and $M_2(u, v)$ represent power series with terms $u^iv^j(i + j \geq 4)$.

Set $\tau = e_1t$, we attain

$$\begin{cases} \frac{du}{d\tau} = u + \frac{e_2}{e_1}u^2 + \frac{e_3}{e_1}uv + \frac{e_4}{e_1}v^2 + \frac{e_5}{e_1}u^3 + \frac{e_6}{e_1}v^3 + \frac{e_7}{e_1}u^2v + \frac{e_8}{e_1}uv^2 + \frac{M_1(u,v)}{e_1} \triangleq u + U(u, v), \\ \frac{dv}{d\tau} = \frac{f_1}{e_1}uv + \frac{f_1}{e_1}v^2 + \frac{f_2}{e_1}u^2v + \frac{2f_2}{e_1}uv^2 + \frac{f_2}{e_1}v^3 + \frac{M_2(u,v)}{e_1} \triangleq N(u, v). \end{cases} \tag{3.13}$$

From $\frac{du}{d\tau} = 0$, we obtain the implicit function

$$u = \varphi_1(v) = -\frac{e_4}{e_1}v^2 - \frac{e_1e_6 - e_3e_4}{e_1^2}v^3 + \cdots,$$

which satisfies $\varphi_1(0) = \varphi_1'(0) = 0$ and $\varphi_1(v) + U(\varphi_1(v), v) = 0$. Then substituting it into the second equation of (3.13), we have

$$\frac{dv}{d\tau} = \frac{f_1}{e_1}v^2 - \frac{f_1e_4 - f_2e_1}{e_1^2}v^3 + O(|v|^4). \tag{3.14}$$

Hence, according to the Theorem 7.1 in Chapter 2 in [31], we have $m = 2$ and $a_m = \frac{\omega}{(1-\alpha)\alpha(1+\eta\alpha)^2} > 0$, so E_2 is a saddle node. That indicates a neighborhood of $S_\varepsilon(E_2)$ is divided into two parts by two separatrices that move away along the left and the right of E_2. One part consists of two hyperbolic sectors and another is a parabolic sector which is on the upper half plane (see Figure 1(*e*)).

Theorem 3.4. *For the positive equilibrium E_3:*

(*i*) *if $\frac{\omega(1+\alpha)}{2+\eta(1+\alpha)} < \sigma < \frac{\omega}{1+\eta}$, then E_3 is locally asymptotically stable;*
(*ii*) *if $\sigma = \frac{\omega(1+\alpha)}{2+\eta(1+\alpha)}$, then E_3 is a center or weak focus;*
(*iii*) *if $\frac{\omega\alpha}{1+\eta\alpha} < \sigma < \frac{\omega(1+\alpha)}{2+\eta(1+\alpha)}$, then E_3 is unstable.*

Proof. The Jacobian matrix J_{E_3} of $E_3(x^*, y^*)$ is

$$J_{E_3} = \begin{pmatrix} x^*(1 - 2x^* + \alpha) & -\frac{1}{K}x^* \\ \frac{\omega y^*}{(1+\eta x^*)^2} & 0 \end{pmatrix}. \tag{3.15}$$

From $x^*(1 - x^*)(x^* - \alpha) - \frac{1}{K}x^*y^* = 0$, we can derive

$$J_{E_3} = \begin{pmatrix} x^*\frac{(1+\alpha)(\omega-\sigma\eta)-2\sigma}{\omega-\sigma\eta} & -\frac{1}{K}x^* \\ \frac{\omega y^*}{(1+\eta x^*)^2} & 0 \end{pmatrix}. \tag{3.16}$$

So the determinant and the trace of Jacobian matrix J_{E_3} are calculated by

$$Det[J_{E_3}] = \frac{\omega x^*y^*}{K(1 + \eta x^*)^2} \text{ and } Tr[J_{E_3}] = x^*\frac{(1 + \alpha)(\omega - \sigma\eta) - 2\sigma}{\omega - \sigma\eta}.$$

When $\frac{\omega\alpha}{1+\eta\alpha} < \sigma < \frac{\omega}{1+\eta}$, $Det[J_{E_3}]$ is positive, but the sign of $Tr[J_{E_3}]$ cannot be obtained directly. If $\frac{\omega(1+\alpha)}{2+\eta(1+\alpha)} < \sigma < \frac{\omega}{1+\eta}$, then $Tr[J_{E_3}] < 0$, that is E_3 is locally asymptotically stable (see Figure 2(*a*)). If $\sigma = \frac{\omega(1+\alpha)}{2+\eta(1+\alpha)}$, then $Tr[J_{E_3}] = 0$, that implies J_{E_3} has a pair of purely imaginary eigenvalues. It confirms that the equilibrium E_3 may be a center, a weak focus or a center focus. We also can easily show that $F(x, y) = -x^3 + (1 + \alpha)x^2 - \frac{1}{K}xy$ and $G(x, y) = \frac{\omega xy}{1+\eta x}$, which are the nonlinear parts of system (1.3), are analytic functions. Thus, from the corollary of Theorem 2.1 in Chapter 4 in [31], we obtain that E_3 is a center (see Figure 2(*b*),(*c*)) or weak focus. If $\frac{\omega\alpha}{1+\eta\alpha} < \sigma < \frac{\omega(1+\alpha)}{2+\eta(1+\alpha)}$, then $Tr[J_{E_3}] > 0$, it means E_3 is unstable (see Figure 2(*d*),(*e*)). Thus, this completes the proof.

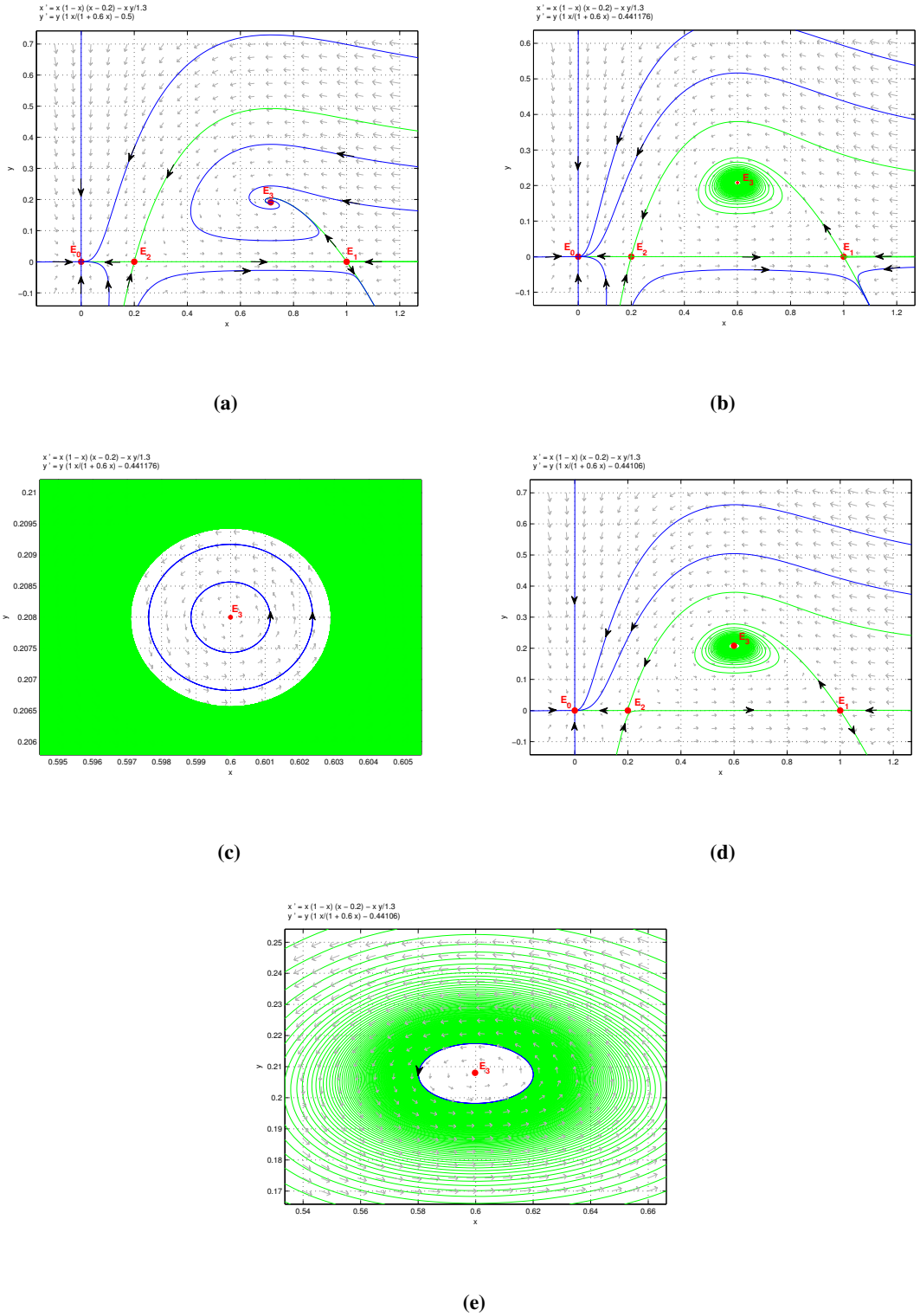

Figure 2. The phase portraits of system (1.3): (a) When $\sigma = 0.5 > \sigma_H$, $E_3(x^*, y^*)$ is locally asymptotically stable; (b) When $\sigma = \sigma_H$, unstable periodic orbits bifurcate through Hopf-bifurcation around $E_3(x^*, y^*)$; (c) Local amplification of (b) for $(x, y) \in [0.595, 0.605] \times [0.206, 0.21]$; (d) When $\sigma = 0.44106 < \sigma_H = 0.441176$, a stable limit cycle appears around $E_3(x^*, y^*)$; (e) Local amplification of (d) for $(x, y) \in [0.54, 0.66] \times [0.17, 0.25]$.

4. Bifurcation analysis

In this part, we mainly put the focus on the various bifurcation behaviors of system (1.3).

4.1. Transcritical bifurcation

Theorem 4.1. *For transcritical bifurcation, the following statements are true.*

(1) *When the parameters satisfy* $\sigma = \sigma_{TC_1} = \frac{\omega}{1+\eta}$, *system* (1.3) *undergoes a transcritical bifurcation referred as* TC_1 *at* E_1*;*
(2) *When the parameters satisfy* $\sigma = \sigma_{TC_2} = \frac{\omega\alpha}{1+\eta\alpha}$, *system* (1.3) *undergoes another transcritical bifurcation referred as* TC_2 *at* E_2.

Proof. (1) Now we verify the transversality condition for transcritical bifurcation by using Sotomayor's theorem [32, 33]. If $\sigma = \sigma_{TC_1} = \frac{\omega}{1+\eta}$, then $Det[J_{E_1}] = 0$, which means one eigenvalue of the Jacobian matrix J_{E_1} is zero. Let V and W represent the two eigenvectors corresponding to the zero eigenvalue of J_{E_1} and it's transpose $J_{E_1}^T$, respectively, and they are given by

$$V = \begin{pmatrix} v_1 \\ v_2 \end{pmatrix} = \begin{pmatrix} 1 \\ K(\alpha - 1) \end{pmatrix} \text{ and } W = \begin{pmatrix} w_1 \\ w_2 \end{pmatrix} = \begin{pmatrix} 0 \\ 1 \end{pmatrix}.$$

Furthermore, we have

$$F_\sigma(E_1; \sigma_{TC_1}) = \begin{pmatrix} 0 \\ -y \end{pmatrix}_{(E_1;\sigma_{TC_1})} = \begin{pmatrix} 0 \\ 0 \end{pmatrix}, \tag{4.1}$$

$$DF_\sigma(E_1; \sigma_{TC_1})V = \begin{pmatrix} 0 & 0 \\ 0 & -1 \end{pmatrix} \begin{pmatrix} 1 \\ K(\alpha - 1) \end{pmatrix}_{(E_1;\sigma_{TC_1})} = \begin{pmatrix} 0 \\ K(\alpha - 1) \end{pmatrix}, \tag{4.2}$$

$$D^2F(E_1; \sigma_{TC_1})(V, V) = \begin{pmatrix} \frac{\partial^2 F_1}{\partial x^2}v_1^2 + 2\frac{\partial^2 F_1}{\partial x \partial y}v_1 v_2 + \frac{\partial^2 F_1}{\partial y^2}v_2^2 \\ \frac{\partial^2 F_2}{\partial x^2}v_1^2 + 2\frac{\partial^2 F_2}{\partial x \partial y}v_1 v_2 + \frac{\partial^2 F_2}{\partial y^2}v_2^2 \end{pmatrix}_{(E_1;\sigma_{TC_1})} = \begin{pmatrix} -2 \\ \frac{2K\omega(\alpha-1)}{(1+\eta)^2} \end{pmatrix}.$$

Also

$$W^T F_\sigma(E_1; \sigma_{TC_1}) = 0,$$

$$W^T \left[DF_\sigma(E_1; \sigma_{TC_1})V\right] = K(\alpha - 1) \neq 0,$$

$$W^T \left[D^2F(E_1; \sigma_{TC_1})(V, V)\right] = \frac{2K\omega(\alpha - 1)}{(1 + \eta)^2} \neq 0.$$

Consequently, system (1.3) undergoes a transcritical bifurcation at $\sigma = \sigma_{TC_1}$.

(2) Now we also apply Sotomayor's theorem to prove the transversality condition for another transcritical bifurcation at $\sigma = \sigma_{TC_2} = \frac{\omega\alpha}{1+\eta\alpha}$. Similar to the process of the former, the transversality condition is derived.

$$W^T F_\sigma(E_2; \sigma_{TC_2}) = 0,$$

$$W^T \left[DF_\sigma(E_2; \sigma_{TC_2})V\right] = -K\alpha(1 - \alpha) \neq 0,$$

and

$$W^T\left[D^2F(E_2;\sigma_{TC_2})(V,V)\right] = \frac{-2K\omega\alpha(1-\alpha)}{(1+\eta)^2} \neq 0,$$

where

$$V = \begin{pmatrix} v_1 \\ v_2 \end{pmatrix} = \begin{pmatrix} 1 \\ K\alpha(1-\alpha) \end{pmatrix} \text{ and } W = \begin{pmatrix} w_1 \\ w_2 \end{pmatrix} = \begin{pmatrix} 0 \\ 1 \end{pmatrix}$$

are the two eigenvectors corresponding to the zero eigenvalue of the Jacobian matrix J_{E_2} and it's transpose $J_{E_2}^T$, respectively. Hence, we complete the proof.

In particular, from Figure 1(a), we can see that for $\sigma < \sigma_{TC_1}$, there are two equilibria E_1 and E_3. And E_1 is unstable and E_3 is stable. For $\sigma = \sigma_{TC_1}$ (see Figure 1(b)), these two equilibria coalesce. For $\sigma > \sigma_{TC_1}$(see Figure 1(c)), E_1 is stable and E_3 is unstable. In this case, E_3 is a negative equilibrium. Biologically, we consider the positive equilibria, so we ignore it in the corresponding phase portrait. Thus, an exchange of stability has occurred at $\sigma = \sigma_{TC_1}$, that is to say, the transcritical bifurcation at $\sigma = \sigma_{TC_1}$ occurs by the Sotomayor's theorem. Moreover, the occurrence of another transcritical bifurcation at $\sigma = \sigma_{TC_2}$ is similarly illustrated in Figure1(d), (e), (f).

4.2. Hopf-bifurcation and the existence of limit cycle

In this subsection, the possible occurrence of Hopf-bifurcation around the interior equilibrium E_3 about the bifurcation parameter σ is explored. In a two dimensional system, it is concluded Hopf-bifurcation occurs as the stability of the interior equilibrium changes (from stable to unstable or vice-versa) and a periodic solution appears (or disappears). Next, we will give the proof of the existence for Hopf-bifurcation of system (1.3).

4.2.1. Hopf-bifurcation

Theorem 4.2. *The conditions for occurrence of Hopf-bifurcation at the critical value* $\sigma = \sigma_H = \frac{\omega(1+\alpha)}{2+\eta(1+\alpha)}$ *around the positive equilibrium* $E_3(x^*, y^*)$ *are* $\frac{\omega\alpha}{1+\eta\alpha} < \sigma < \frac{\omega}{1+\eta}$ *and* $\frac{d}{d\sigma}Tr[J_{E_3}] \neq 0$ *at* $\sigma = \sigma_H$.

Proof. From the Jacobian matrix J_{E_3} calculated at $E_3(x^*, y^*)$, we consider σ as a bifurcation parameter. For occurrence of Hopf-bifurcation, the characteristic equation of J_{E_3} must have a pair of purely imaginary roots. At $\sigma = \sigma_H$, $Tr[J_{E_3}] = 0$, then the characteristic equation of J_{E_3} becomes

$$\lambda^2 + Det[J_{E_3}] = 0. \tag{4.3}$$

When $\frac{\omega\alpha}{1+\eta\alpha} < \sigma < \frac{\omega}{1+\eta}$, $Det[J_{E_3}] > 0$, namely the above characteristic equation has a pair of conjugated imaginary eigenvalues $\lambda_{1,2} = \pm i\theta$, where $\theta = \sqrt{Det[J_{E_3}]}$.

Now we check the transversality condition $\frac{d}{d\sigma}\{Re(\lambda)\}|_{\sigma=\sigma_H} \neq 0$ which confirms the eigenvalues cross the imaginary axis transversely with non-zero speed. Let σ be any point in the neighbourhood of σ_H, the eigenvalues of the Jacobian matrix J_{E_3} at σ are $\lambda_{1,2} = \chi(\sigma) \pm i\theta(\sigma)$, where $\chi(\sigma) = \frac{Tr[J_{E_3}]}{2}$ and $\theta(\sigma) = \sqrt{Det[J_{E_3}] - \frac{Tr^2[J_{E_3}]}{4}}$. Then

$$\frac{d}{d\sigma}\{Re(\lambda)\}|_{\sigma=\sigma_H} = \frac{d}{d\sigma}\chi(\sigma)|_{\sigma=\sigma_H} = \frac{d}{2d\sigma}Tr[J_{E_3}]|_{\sigma=\sigma_H} = \frac{3}{48\omega}(1+\alpha)(2+(1+\alpha)\eta)^2 \neq 0. \tag{4.4}$$

Thus the transversality condition is verified and a Hopf-bifurcation of system (1.3) occurs at $\sigma = \sigma_H$.

4.2.2. Direction of Hopf-bifurcation

In order to determine the direction of Hopf-bifurcation and the stability of the periodic solution which originates from the positive equilibrium via Hopf bifurcation, the first Lyapunov coefficient [33] needs to be computed.

Firstly, set $z_1 = x - x^*$ and $z_2 = y - y^*$, then system (1.3) can be written as

$$\begin{cases} \dot{z_1} = m_{10}z_1 + m_{01}z_2 + m_{20}z_1^2 + m_{11}z_1z_2 + m_{02}z_2^2 + m_{30}z_1^3 + m_{21}z_1^2z_2 + m_{12}z_1z_2^2 + m_{03}z_2^3, \\ \dot{z_2} = n_{10}z_1 + n_{01}z_2 + n_{20}z_1^2 + n_{11}z_1z_2 + n_{02}z_2^2 + n_{30}z_1^3 + n_{21}z_1^2z_2 + n_{12}z_1z_2^2 + n_{03}z_2^3 + O_1(z_1, z_2), \end{cases} \tag{4.5}$$

where

$$\begin{aligned} &m_{10} = (1 - 2x^* + \alpha)x^*,\ m_{01} = -\frac{1}{K}x^*,\ m_{20} = 1 - 3x^* + \alpha,\ m_{11} = -\frac{1}{K},\ m_{02} = 0, \\ &m_{30} = -1,\ m_{21} = m_{12} = m_{03} = 0,\ n_{10} = \frac{\omega y^*}{(1+\eta x^*)^2},\ n_{01} = 0,\ n_{20} = -\frac{\omega\eta y^*}{(1+\eta x^*)^3}, \\ &n_{11} = \frac{\omega}{(1+\eta x^*)^2},\ n_{02} = 0,\ n_{30} = -\frac{\omega\eta^2 y^*}{(1+\eta x^*)^4},\ n_{21} = -\frac{\omega\eta}{(1+\eta x^*)^3},\ n_{12} = n_{03} = 0. \end{aligned}$$

By ignoring the higher order terms of degree 4 and above, then system (4.5) becomes

$$\dot{Z} = J_{E_3}Z + A(Z), \tag{4.6}$$

where

$$Z = \begin{pmatrix} Z_1 \\ Z_2 \end{pmatrix} \text{and } A = \begin{pmatrix} A_1 \\ A_2 \end{pmatrix} = \begin{pmatrix} m_{20}z_1^2 + m_{11}z_1z_2 + m_{02}z_2^2 + m_{30}z_1^3 \\ +m_{21}z_1^2z_2 + m_{12}z_1z_2^2 + m_{03}z_2^3 \\ n_{20}z_1^2 + n_{11}z_1z_2 + n_{02}z_2^2 + n_{30}z_1^3 \\ +n_{21}z_1^2z_2 + n_{12}z_1z_2^2 + n_{03}z_2^3 \end{pmatrix}.$$

The eigenvector $\bar{v}$ of J_{E_3} for the eigenvalue $i\theta$ at $\sigma = \sigma_H$ is $\bar{v} = \begin{pmatrix} m_{01} \\ i\theta - m_{10} \end{pmatrix}$.

Now we define

$$Q = (Re(\bar{v}), -Im(\bar{v})) = \begin{pmatrix} m_{01} & 0 \\ -m_{10} & -\theta \end{pmatrix}.$$

Let $Z = QU$, where $U = \begin{pmatrix} u \\ v \end{pmatrix}$. Under this transformation, system (4.6) becomes

$$\dot{U} = (Q^{-1}J_{E_3}Q)U + A(QU).$$

Thus

$$\begin{pmatrix} \dot{u} \\ \dot{v} \end{pmatrix} = \begin{pmatrix} 0 & -\theta \\ \theta & 0 \end{pmatrix} = \begin{pmatrix} u \\ v \end{pmatrix} + \begin{pmatrix} S^1(u, v; \sigma = \sigma_H) \\ S^2(u, v; \sigma = \sigma_H) \end{pmatrix}, \tag{4.7}$$

where S^1 and S^2 are non-linear in u and v given by

$$S^1(u, v; \sigma = \sigma_H) = \frac{1}{m_{01}A_1},\ \ S^2(u, v; \sigma = \sigma_H) = -\frac{1}{\theta m_{01}}(m_{10}A_1 + m_{01}A_2)$$

with

$$\begin{aligned}
A_1 =&(m_{20}m_{01}^2 - m_{11}m_{01}m_{10} + m_{02}m_{10}^2)u^2 + \theta(2m_{02}m_{10} - m_{11}m_{01})uv + \theta^2 m_{02}v^2\\
&+ (m_{12}m_{01}m_{10}^2 - m_{03}m_{10}^3 + m_{30}m_{01}^3 - m_{21}m_{01}^2m_{10})u^3\\
&+ \theta(2m_{12}m_{10}m_{01} - m_{21}m_{01}^2 - 3m_{03}m_{10}^2)u^2v\\
&+ \theta^2(m_{12}m_{01} - 3m_{03}m_{10})uv^2 - \theta^3 m_{03}v^3,\\
A_2 =&(n_{20}m_{01}^2 - n_{11}m_{01}m_{10} + n_{02}m_{10}^2)u^2 + \theta(2n_{02}m_{10} - n_{11}m_{01})uv + \theta^2 n_{02}v^2\\
&+ (n_{12}m_{01}m_{10}^2 - n_{03}m_{10}^3 + n_{30}m_{01}^3 - n_{21}m_{01}^2m_{10})u^3\\
&+ \theta(2n_{12}m_{10}m_{01} - n_{21}m_{01}^2 - 3n_{03}m_{10}^2)u^2v\\
&+ \theta^2(n_{12}m_{01} - 3n_{03}m_{10})uv^2 - \theta^3 n_{03}v^3.
\end{aligned}$$

Regarding the normal form (4.7), we calculate the first Lyapunov coefficient and obtain

$$\begin{aligned}
l_1 =& \frac{1}{16}\left(S^1_{uuu} + S^1_{uvv} + S^2_{vvv}\right)\\
&+ \frac{1}{16\theta}\left(S^1_{uv}(S^1_{uu} + S^1_{vv}) - S^2_{uv}(S^2_{uv} + S^2_{vv}) - S^1_{uu}S^2_{uu} + S^1_{vv}S^2_{vv}\right)\\
=& \frac{1}{16}\left(6m_{30}m_{01}^2 + 2n_{21}m_{01}^2\right) + \frac{1}{16\theta}\left(-2\omega m_{20}m_{01} + \frac{2}{\theta}n_{11}n_{20}m_{01}^3 + \frac{4}{\theta}n_{20}m_{20}m_{01}^3\right)\\
=& -\frac{1}{4}x^{*2}\left(\frac{1}{K^2} + \frac{x^{*2}}{K^3(1+\eta x^*)}\right).
\end{aligned}$$

Evidently, $l_1 < 0$, so that a stable Hopf-bifurcating limit cycle appears and the Hopf-bifurcation is supercritical, which indicates the stable periodic solution overlaps an unstable interior equilibrium. From view of ecology, this phenomenon means that both predators and prey reach an oscillatory coexistence state. And, in the next section, we are going to explore this phenomenon a step further with the help of numerical simulations.

5. Numerical simulation and discussion

To verify the validity of the obtained analytical results, in this part, some numerical simulations and computations are carried out. Firstly, the phase portraits corresponding to the scenario of no positive equilibrium and one positive equilibrium are plotted in Figures 1 and 2 by varying the key parameter value σ and keeping other fixed parameters values $\alpha = 0.2$, $K = 1.3$, $\omega = 1$ and $\eta = 0.6$. Further, using this set of parameter values and different values of σ, we also give some time series diagrams of system (1.3) for a better visualization of how the strong Allee effect influence the dynamics of the model, with special attention to the stability and cyclical behavior.

Case 5.1. For σ=0.5, the high mortality of natural enemy predator, prey and the natural enemy populations reach a stable coexistence state because of the reduced predation pressure on prey and Allee effect (Figures 2(a) and 3).

Case 5.2. For gradually decreasing the value of σ, the positive equilibrium E_3 of model (1.3) loses stability via a Hopf bifurcation at σ_H=0.441176 (Figure 2(b),(c)) and the Hopf bifurcation is supercritical as the first Lyapunov coefficient $l_1 = -0.072449680827 < 0$. Meanwhile, as shown in Figure 4, both the total populations begin to oscillate. From Figure 2(d),(e), it is found when $\sigma < \sigma_H$ slightly, a stable limit cycle from E_3 is bifurcated. Prey and predator populations reach an

oscillation coexistence state (Figure 5). The amplitude of the oscillation is initially small, but then increases rapidly with decreasing σ, which is illustrated with a three-dimensional bifurcation diagram in Figure 6. Biologically, the populations fluctuate a lot, which corresponds to the sudden increase of prey.

Case 5.3. For small value σ=0.3, the low mortality of natural enemy predator, we observe that the limit cycle disappears and both prey and predator approach the extinction state for the higher predation pressure on prey and the Allee effect (Figures 1(f) and 7).

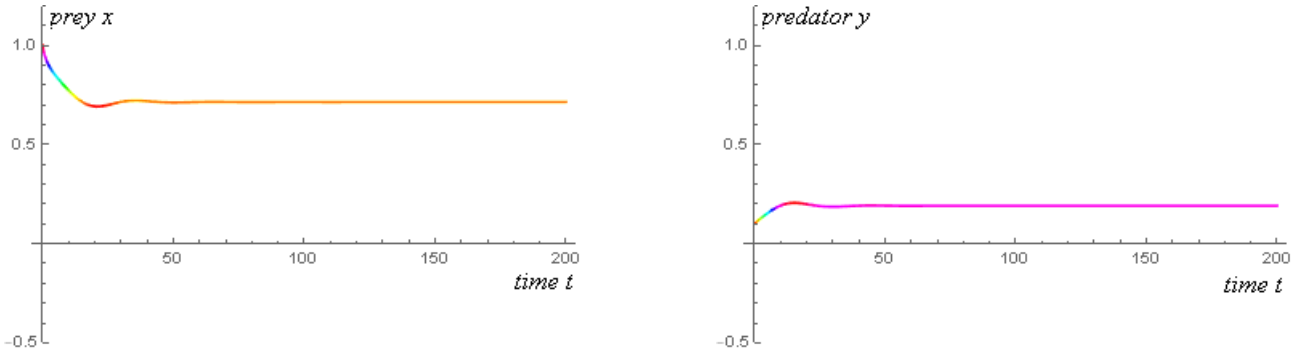

(a) **(b)**

Figure 3. The time series diagram of system (1.3) for σ=0.5 with the initial condition $[x(0), y(0)]$=[1, 0.1].

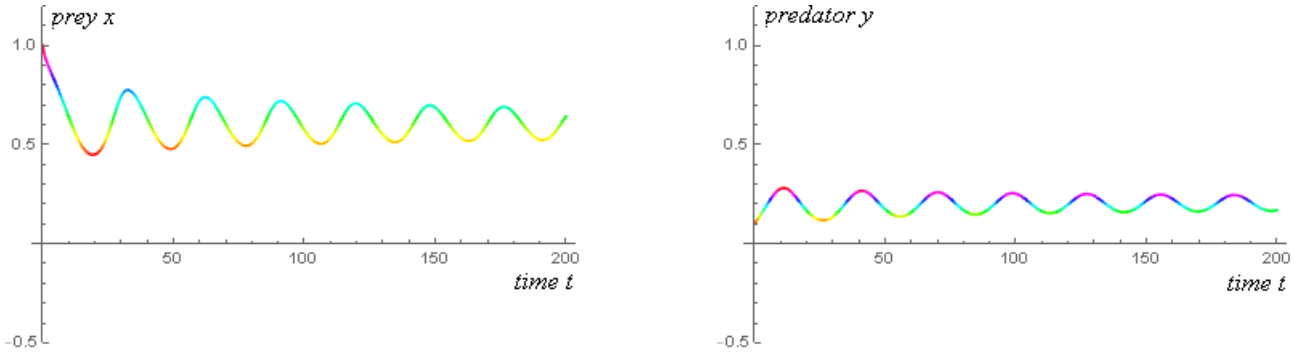

(a) **(b)**

Figure 4. The time series diagram of system (1.3) for σ_H=0.441176 with the initial condition $[x(0), y(0)]$=[1, 0.1]

.

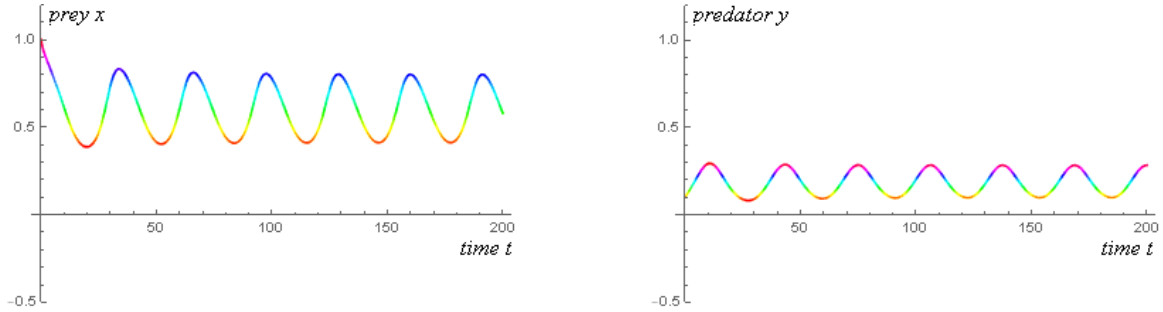

(a) **(b)**

Figure 5. The time series diagram of system (1.3) for σ=0.44106 with the initial condition $[x(0), y(0)]$=[1, 0.1].

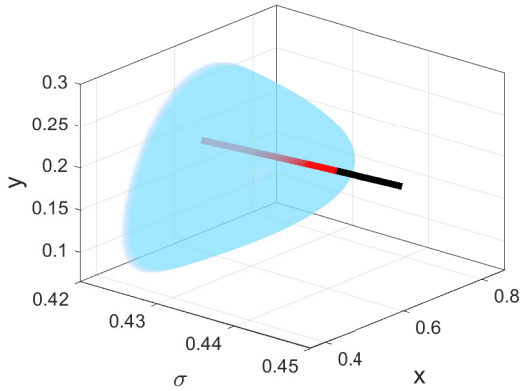

Figure 6. The three-dimensional space bifurcation diagram with $\sigma \in [0.42, 0.45]$, where the black curve represents unstable equilibria, the red curve represents the stable equilibria and the blue surface denotes the stable limit cycle.

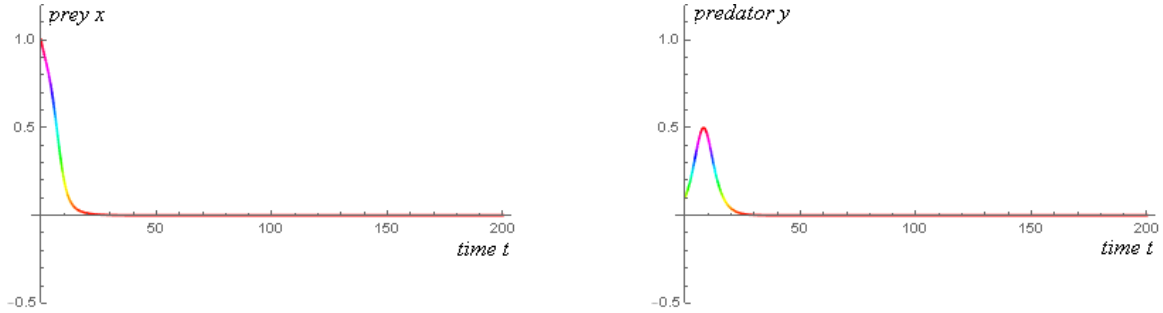

(a) **(b)**

Figure 7. The time series diagram of system (1.3) for σ=0.3 with the initial condition $[x(0), y(0)]$=[1, 0.1].

Remark 5.1. One can see that the model is sensitive to the initial condition. The strong Allee effect causes more complex dynamics, with total population density tending to either the extinction state $E_0(0,0)$ or coexistence state $E_3(x^*, y^*)$ depending on the selection of the initial condition. In the real world, for biological protection, our purpose is generally to maintain the sustainable survival of species rather than eradicating the species completely. Accordingly, in the above cases, we choose the initial condition $[x(0), y(0)]$=[1, 0.1].

6. Conclusions

In this article, a predator-prey model with strong Allee effect in prey was proposed. We investigated the classification and stability of each equilibrium of system (1.3) and fulfilled a comprehensive bifurcation analysis. Qualitative analysis shows that the model's dynamics grow more complicated when Allee effect is incorporated into the first species. More specifically, with the comparison to system (1.1) [28] in absence of Allee effect, we find some new dynamical properties of model (1.3).

(1) System (1.3) possesses more types of equilibria due to the strong Allee effect. The extinction equilibrium is always an attractor, whereas the stability of other two boundary equilibria and the unique interior equilibrium changes with different parameter conditions. For the system with no Allee effect, both boundary equilibria are saddles and the interior equilibrium is always globally asymptotically stable.

(2) System (1.3) exhibits more bifurcation behaviors for the existence of multiple types of equilibria. Only one transcritical bifurcation occurs for system (1.1), whereas system (1.3) undergoes two transcritical bifurcations and one Hopf-bifurcation. Also a stable limit cycle around unstable positive equilibrium E_3 corresponding to system (1.3) appears.

It can be clearly seen that the strong Allee effect can lead to potential changes in system dynamics. It also has a significant role in ecology. Allee effect, such as, can destabilize the coexistence steady state. From stable coexistence to oscillating coexistence, and then from oscillating coexistence to overall populations extinction state, the prey and predator populations go through multiple stability switches. Moreover, in all cases, the possibility of total species extinction in the model is caused by Allee effect. This suggests that if prey or predators are subject to Allee effect, the measures we adopt for nature preservation should take this into consideration, which is important for analyzing the long-term survival of all populations.

We just consider the impact of Allee effect in prey on the dynamical behaviors of the predator-prey system in this paper. It will be an interesting theme to study the dynamics of the model with Allee effects in both populations. We will leave this as future work.

Acknowledgments

The second author was supported by the National Natural Science Foundation of China (No.12001503) and the third author was supported by the Project of Beijing Municipal Commission of Education (KM 202110015001).

Conflict of interest

The authors declare no conflict of interest.

References

1. N. Bacaer, *A short history of mathematical population dynamics*, Springer London, 2011.
2. S. Bentout, A. Tridane, S. Djilali, T. M. Touaoula, Age-structured modeling of COVID-19 epidemic in the USA, UAE and Algeria, *Alex. Eng. J.,* **60** (2021), 401–411. https://doi.org/10.1016/j.aej.2020.08.053
3. S. Djilali, S. Bentout, S. Kumar, T. M. Touaoula, Approximating the asymptomatic infectious cases of the COVID-19 disease in Algeria and India using a mathematical model, *Int. J. Model. Simul. SC,* **2250028** (2022).
4. A. Singh, A. Parwaliya, A. Kumar, Hopf bifurcation and global stability of density-dependent model with discrete delays involving Beddington-DeAngelis functional response, *Math. Method. Appl. Sci.,* **44** (2021), 8838–8861. https://doi.org/10.1002/mma.7311
5. A. Singh, P. Malik, Bifurcations in a modified Leslie-Gower predator-prey discrete model with Michaelis-Menten prey harvesting, *J. Appl. Math. Comput.,* **67** (2021), 143–174. https://doi.org/10.1007/s12190-020-01491-9
6. H. I. Freedman, Stability analysis of a predator-prey system with mutual interference and density-dependent death rates, *Bull. Math. Biol.,* **41** (1979), 67–78. https://doi.org/10.1016/S0092-8240(79)80054-3
7. D. P. Hu, H. J. Cao, Stability and bifurcation analysis in a predator-prey system with Michaelis-Menten type predator harvesting, *Nonlinear Anal.-Real,* **33** (2017), 58–82. https://doi.org/10.1016/j.nonrwa.2016.05.010
8. L. Li, W. C. Zhao, Deterministic and stochastic dynamics of a modified Leslie-Gower prey-predator system with simplified Holling-type IV scheme, *Math. Biosci. Eng.,* **18** (2021), 2813–2831. https://doi.org/10.3934/mbe.2021143
9. S. Djilali, S. Bentout, Spatiotemporal patterns in a diffusive predator-prey model with prey social behavior, *Acta. Appl. Math.,* **169** (2020), 1–19. https://doi.org/10.1007/s10440-019-00291-z
10. S. Djilali, S. Bentout, Pattern formations of a delayed diffusive predator-prey model with predator harvesting and prey social behavior, *Math. Method. Appl. Sci.,* **44** (2021), 9128–9142. https://doi.org/10.1002/mma.7340
11. M. J. Groom, Allee effects limit population viability of an annual plant, *Am. Nat.,* **151** (1998), 487–496. https://doi.org/10.1086/286135
12. M. Kuussaari, I. Saccheri, M. Camara, I. Hanski, Allee effect and population dynamics in the Glanville fritillary butterfly, *Oikos,* **82** (1998), 384–392. https://doi.org/10.2307/3546980
13. F. Courchamp, T. Clutton-Brock, B. Grenfell, Inverse density dependence and the Allee effect, *Trends Ecol. Evol.,* **14** (1999), 405–410. https://doi.org/10.1016/S0169-5347(99)01683-3

14. M. A. Mccarthy, The Allee effect, finding mates and theoretical models, *Ecol. Model.,* **103** (1997), 99–102. https://doi.org/10.1016/S0304-3800(97)00104-X

15. F. Courchamp, L. Berec, J. Gascoigne, *Allee effects in ecology and conservation,* Oxford University Press, London, 2008. https://doi.org/10.1093/acprof:oso/9780198570301.001.0001

16. M. Wang, M. Kot, Speeds of invasion in a model with strong or weak Allee effects, *Math. Biosci.,* **171** (2001), 83–97. https://doi.org/10.1016/S0025-5564(01)00048-7

17. J. F. Wang, J. P. Shi, J. J. Wei, Predator-prey system with strong Allee effect in prey, *J. Math. Biol.,* **62** (2011), 291–331. https://doi.org/10.1007/s00285-010-0332-1

18. U. Kumar, P. S. Mandal, E. Venturino, Impact of Allee effect on an eco-epidemiological system, *Ecol. Complex.,* **42** (2020), 100828. https://doi.org/10.1016/j.ecocom.2020.100828

19. G. Voorn, L. Hemerik, M. P. Boer, B. W. Kooi, Heteroclinic orbits indicate over exploitation in predator-prey systems with a strong Allee effect, *Math. Biosci.,* **209** (2007), 451–469. https://doi.org/10.1016/j.mbs.2007.02.006

20. F. M. Hilker, M. Langlais, H. Malchow, The Allee effect and infectious diseases: Extinction, multistability, and the (dis)appearance of oscillations, *Am. Nat.,* **173** (2009), 72–88. https://doi.org/10.1086/593357

21. S. Bentout, A. Chekroun, T. Kuniya, Parameter estimation and prediction for coronavirus disease outbreak 2019 (COVID-19) in Algeria, *AIMS Public Health,* **7** (2020), 306–318. https://doi.org/10.3934/publichealth.2020026

22. S. Bentout, T. M. Touaoula, Global analysis of an infection age model with a class of nonlinear incidence rates, *J. Math. Anal. Appl.,* **434** (2016), 1211–1239. https://doi.org/10.1016/j.jmaa.2015.09.066

23. S. Djilali, A. Mezouaghi, O. Belhamiti, Bifurcation analysis of a diffusive predator-prey model with schooling behaviour and cannibalism in prey, *Int. J. Math. Model. Numer. Opt.,* **11** (2021), 209. https://doi.org/10.1504/IJMMNO.2021.116676

24. J. Zu, M. Mimura, The impact of Allee effect on a predator-prey system with Holling type II functional response, *Appl. Math. Comput.,* **217** (2010), 3542–3556. https://doi.org/10.1016/j.amc.2010.09.029

25. C. S. Holling, The functional response of predators to prey density and its role in mimicry and population regulation, *Mem. Entomol. Soc. Can.,* **97** (1965), 1–60. https://doi.org/10.4039/entm9745fv

26. S. Y. Tang, Y. N. Xiao, L. S. Chen, Integrated pest management models and their dynamical behaviour, *Bull. Math. Biol.,* **67** (2005), 115–135. https://doi.org/10.1016/j.bulm.2004.06.005

27. J. Zu, W. D. Wang, B. Zu, Evolutionary dynamics of prey-predator systems with Holling type II, *Math. Biosci. Eng.,* **4** (2007), 221–237. https://doi.org/10.3934/mbe.2007.4.221

28. K. B. Sun, T. H. Zhang, Y. Tian, Dynamics analysis and control optimization of a pest management predator-prey model with an integrated control strategy, *Appl. Math. Comput.,* **292** (2017), 253–271. https://doi.org/10.1016/j.amc.2016.07.046

29. K. X. Wang, Influence of feedback controls on the global stability of a stochastic predator-prey model with Holling type II response and infinite delays, *Discrete. Cont. Dyn.-B,* **25** (2020), 1699–1714. https://doi.org/10.3934/dcdsb.2019247

30. X. Y. Wu, H. Zheng, S. C. Zhang, Dynamics of a non-autonomous predator-prey system with Hassell-Varley-Holling II function response and mutual interference, *AIMS Math.,* **6** (2021), 6033–6049. https://doi.org/10.3934/math.2021355

31. Z. F. Zhang, T. R. Ding, W. Z. Huang, Z. X. Dong, *Qualitative theory of differential equation,* Science Press, Beijing, 1997.

32. J. Sotomayor, *Dynamical systems: Generic bifurcations of dynamical systems,* Academic Press, New York, 1973, 561–582. https://doi.org/10.1016/B978-0-12-550350-1.50047-3

33. L. Perko, *Differential equations and dynamical systems,* Springer, New York, 2001.

AIMS Press